



Article

Solvent-Dependent Fluorescence Properties of CH₂-bis(BODIPY)s

Alexander Kalyagin, Lubov Antina, Alexander Ksenofontov , Elena Antina * and Mikhail Berezin

G.A. Krestov Institute of Solution Chemistry of the Russian Academy of Sciences, 1 Akademicheskaya Str., 153045 Ivanovo, Russia

* Correspondence: eva@isc-ras.ru

Abstract: Biocompatible luminophores based on organic dyes, which have fluorescence characteristics that are highly sensitive to the properties of the solvating medium, are of particular interest as highly sensitive, selective, and easy-to-use analytical agents. We found that BODIPY dimers (2,2'-, 2,3'-3,3'-CH₂-bis(BODIPY) (1–3)) demonstrate fluorescence characteristics with a high sensitivity to the presence of polar solvents. The intense fluorescence of 1–3 in nonpolar/low-polarity solvents is dramatically quenched in polar media (acetone, DMF, and DMSO). It has been established that the main reason for CH₂-bis(BODIPY) fluorescence quenching is the specific solvation of dyes by electron-donating molecules (Solv) with the formation of stable supramolecular CH₂-bis(BODIPY)·2Solv structures. Using steady-state absorption and fluorescence spectroscopy, time-resolved fluorescence spectroscopy, and computational modeling, the formation mechanism, composition, and structure of CH₂-bis(BODIPY)·2Solv supramolecular complexes have been substantiated, and their stability has been evaluated. The results show the promise of developing fluorescent probes based on CH₂-bis(BODIPY)s for detecting toxic N/O-containing compounds in solutions.

Keywords: CH₂-bis(BODIPY); fluorescent sensor; supramolecular structures; computational modelling



Citation: Kalyagin, A.; Antina, L.; Ksenofontov, A.; Antina, E.; Berezin, M. Solvent-Dependent Fluorescence Properties of CH₂-bis(BODIPY)s. *Int. J. Mol. Sci.* **2022**, *23*, 14402. <https://doi.org/10.3390/ijms232214402>

Academic Editors: Lucia Ya. Zakharova and Ruslan R. Kashapov

Received: 14 October 2022

Accepted: 17 November 2022

Published: 19 November 2022

Publisher's Note: MDPI stays neutral with regard to jurisdictional claims in published maps and institutional affiliations.



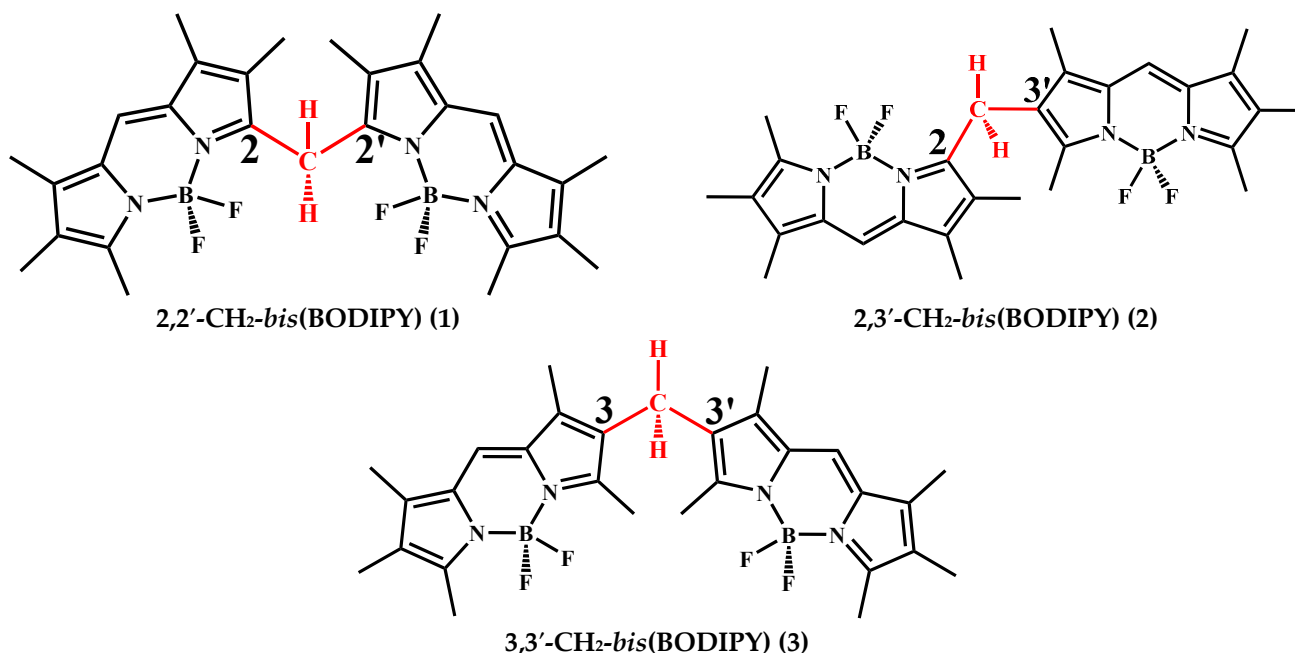
Copyright: © 2022 by the authors. Licensee MDPI, Basel, Switzerland. This article is an open access article distributed under the terms and conditions of the Creative Commons Attribution (CC BY) license (<https://creativecommons.org/licenses/by/4.0/>).

1. Introduction

Fluorescence spectroscopy is an attractive method for detecting specific analytes, including those in biological objects: the non-invasive early diagnosis of cancer, dysplastic lesions, and a number of other diseases [1–5]. In particular, regular contact with toxic N- and O-containing toxic compounds inevitably causes the disruption of important biological processes in the body, which must be detected early. Therefore, the study of compounds with fluorescence sensitivity to polar N- and O-electron-donor analytes is an urgent task. BODIPYs are among the successful candidates as fluorescent probes for analytes various types, such as toxic compounds, the polarity and nature of the medium, viscosity, etc. [6–10]. BODIPY derivatives, including oligomers with two or more BODIPY domains, have gained great interest due to their excellent optical properties, which can be purposefully controlled by modifying the chromophore molecular structure [11–14]. Thus, BODIPY dyes have many potential applications, both as components of optical devices and in bioimaging, photodynamic therapy, and sensorics [8,14–20].

Previous studies by our group [18] have focused on BODIPY dimers with a methylene spacer between the BODIPY domains. We have shown that the exciton splitting of the intense band in the electronic absorption spectra is typical not only for bis(BODIPY)s with a direct covalent bond between BODIPY domains [19–31] but also for CH₂-bis(BODIPY) 1–3 dyes (Scheme 1) with chromophoric domains linked by a methylene group. In contrast to the moderately insensitive fluorescence characteristics of BODIPY monomeric dyes, the fluorescence quantum yield (Φ_f) of dimeric CH₂-bis(BODIPY) luminophores decreases by one or two orders of magnitude in the presence of polar proton- or electron-donating compounds in solutions. The fluorescence quantum yield of alkyl-substituted

CH_2 -bis(BODIPY)s 1–3 decreases from 0.99 in nonpolar cyclic and linear hydrocarbons to 0.06 in polar proton-donor solvents and even to 0.008 in electron-donor organic solvents [21]. Thus, the sensitivity of CH_2 -bis(BODIPY)s 1–3's fluorescence characteristics to the environment's nature is not inferior to the previously studied zinc(II) bis(dipyrromethate)s [22–24] and dimers with a direct covalent bond between the BODIPY domains [25–28].



Scheme 1. Chemical structures of BODIPY dimers (2,2'-, 2,3'-, 3,3'- CH_2 -bis(BODIPY) (1–3)).

Previously, we showed [29] that in alcohols, the increase in the intensity of non-radiative energy losses by molecules 1–3 in the excited state is caused by the formation of CH_2 -bis(BODIPY)·2alcohol supramolecular structures. The slight sensitivity of 1–3's fluorescence to viscosity is observed in highly viscous polar protic media. In the present work, a comprehensive analysis of fluorescence characteristics of 1–3 dimers with high sensitivity to the presence of electron-donating compounds was carried out using steady-state absorption and fluorescence spectroscopy, time-resolved fluorescence spectroscopy, and computational modeling.

2. Results and Discussion

2.1. Effect of the Nature of Polar Electron-Donating Solvents on CH_2 -bis(BODIPY)s 1–3 Spectral Properties

CH_2 -bis(BODIPY)s are characterized by intense absorption band splitting due to the intramolecular exciton interaction of non-conjugated BODIPY moieties [21] (Figure 1a and Table S1). The solvent nature does not significantly affect the absorption and emission bands position of compounds 1–3. The most sensitive spectral characteristic of 1–3 to the medium's nature was the fluorescence quantum yield (Figure 1b). The values of 1–3's fluorescence quantum yield range from 0.008 to 0.99 in the studied media (Table S1). The highest Φ_f values of 1–3 dyes are observed in saturated and aromatic hydrocarbons (cyclohexane, heptane, benzene, and toluene) and chloroform [21]. This is due to the low polarity (polarizability) of these solvents, which solvate solutes only through universal interactions, in contrast to proton-donor (alcohols) and electron-donor solvents.

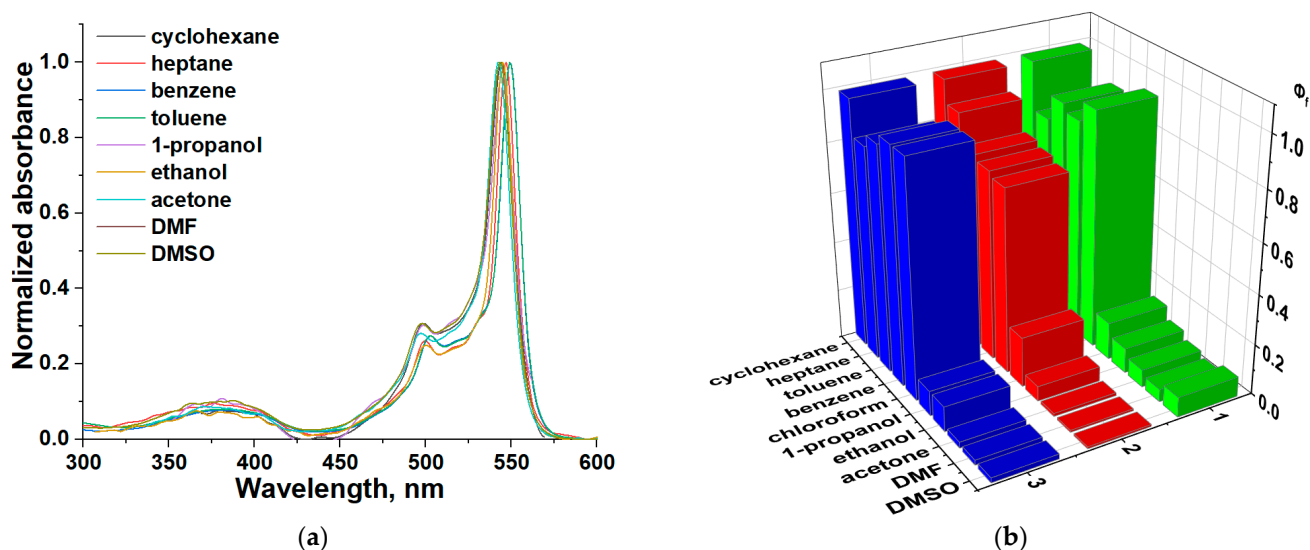


Figure 1. Normalized electronic absorption spectra of **3** in different solvents (a). The fluorescence quantum yield of **1–3** in nonpolar and polar solvents (b).

For comparison, the spectra and fluorescence quantum yield of **1–3** are given in non-polar and polar proton-donating and electron-donating solvents (Figure 1a,b and Table S1). For the three structural isomers of CH_2 -bis(BODIPY), the same fluorescence-quenching trend is observed in alcohols [29], acetone, DMF, and DMSO. However, the fluorescence-quenching efficiency depends significantly on the polar solvent nature. Compared to cyclohexane, the Φ_f of **1–3** decreases by 17 times in alcohols. However, maximum fluorescence quenching (up to 124 times) is observed in electron-donating media.

It is known [30] that the solvating environment's effect on the change in the electronic levels of a molecule can be realized through two types of mechanisms. The first is based on macro-effects due to the macro-properties of solvents: the refractive index of the medium (n), dielectric constant (ϵ), viscosity (η), etc. The second type of dye fluorescence quenching is caused by specific interactions in the nearby solvate environment (donor–acceptor, hydrogen bonds, and π -stacking). We paid attention to the most informative electron-donating solvent parameters: basicity, electron-donating ability, and polarity. For compounds **1–3**, the correlation dependences of Φ_f on various characteristics of solvents were plotted: Gutmann donor number (DN); Catalan's solvent parameters: basicity (SB) and solvent polarity/polarizability (SPP); Kamlet–Taft solvent parameters: empirical parameter of solvent hydrogen-bond acceptor basicity (β) and dipolarity/polarizability parameters (π^*); dielectric constant (ϵ); and dipole moment (μ) (Figure S1 and Table S2). Irrespective of the chosen scale, in all cases, the same trend of a decrease in the fluorescence quantum yield with an increase in the polarity, basicity, and electron-donor properties of the solvent was observed. The plots of Φ_f vs. the solvent parameters (DN , SB , SPP , β , π^* , ϵ , and μ) (Figure S1) deviate from linearity. Therefore, the high sensitivity of **1–3**'s luminescent characteristics to the solvent nature is due not only to the universal solvation of dye molecules by more polar and polarizable solvents but mainly to specific interactions between solvent molecules and the luminophores.

The results of time-resolved fluorescence spectroscopy confirm this assumption (Figure 2; Tables S1 and S3). In inert solvents (heptane or benzene), the decay curves are monoexponential. In electron-donor solvents (acetone, DMF, or DMSO (Figure 2a–c)), the decay curves are biexponential. This may indicate the presence of an equilibrium mixture of the initial CH_2 -bis(BODIPY) complex and its specifically solvated form, CH_2 -bis(BODIPY)· $n\text{Solv}$, with a low fluorescence lifetime in the solution. The supramolecular complex with a short fluorescence lifetime (from 0.023 to 0.15 ns, Table S3) makes the maximum contribution to the total fluorescence lifetime. This indicates a significant shift of the equilibrium towards stable solvate structures of CH_2 -bis(BODIPY)· $n\text{Solv}$.

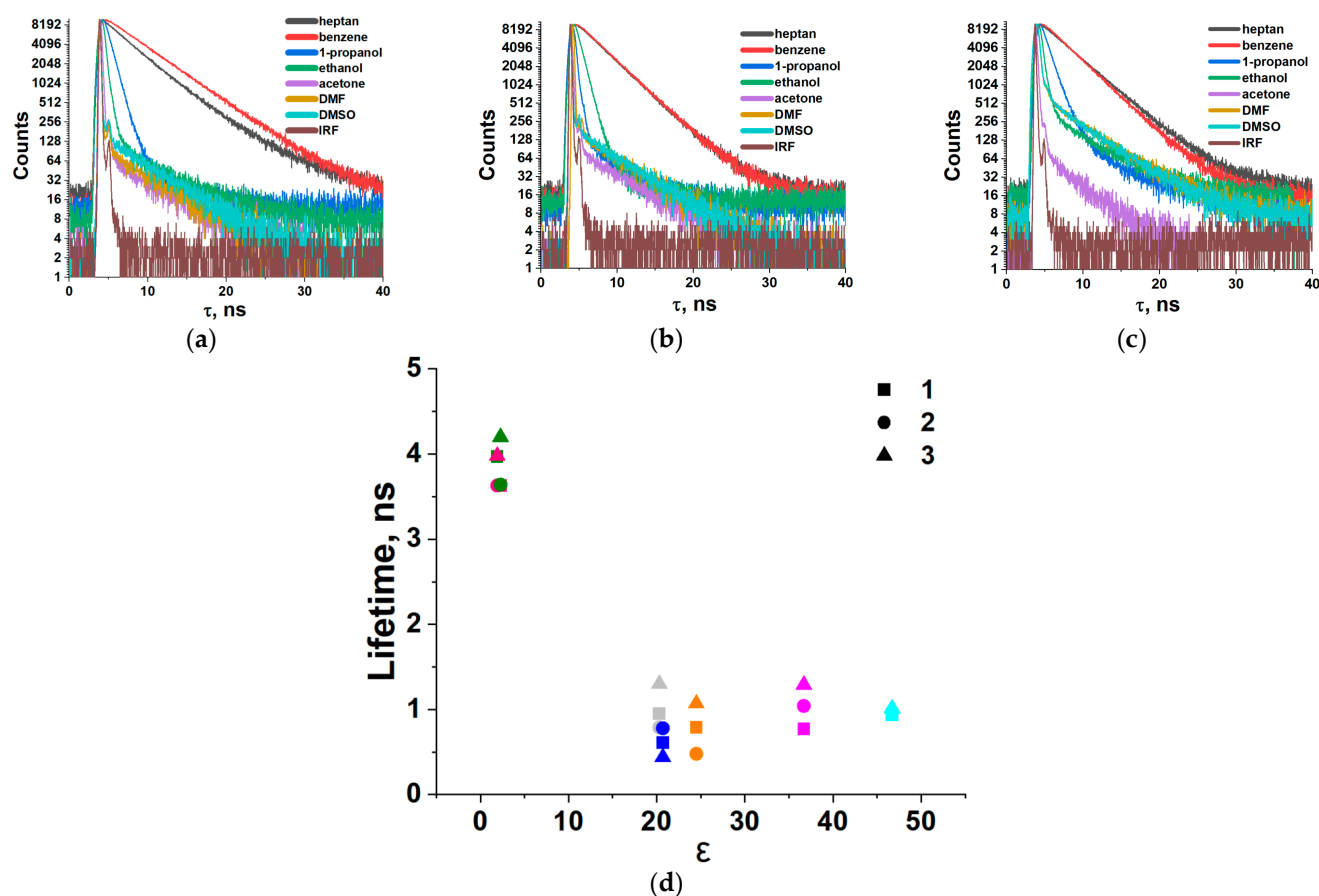


Figure 2. Time-resolved fluorescence decays of **1–3** in organic solvents (a–c) and the dependences of fluorescence lifetimes of **1–3** on organic solvent dielectric constant (d). ●—heptane; ●—benzene; ●—1-propanol; ●—ethanol; ●—acetone; ●—DMF; ●—DMSO.

In Table S1, the values of the total lifetime and the calculated [30] radiative and non-radiative constants are given. The results show that for all **1–3** dyes in nonpolar media, the lifetime is noticeably longer (3.17–4.2 ns) than in acetone, DMF, and DMSO (0.44–1.30 ns). The value of the non-radiative constant is an order of magnitude higher in electron-donating solvents than in nonpolar media (Table S2). Obviously, in polar electron-donating solvents, non-radiative processes associated with rearrangements in the CH_2 -*bis*(BODIPY) solvation shell formed due to the active universal and specific interactions of the luminophores with the solvent molecules (Solv). The composition and stability of CH_2 -*bis*(BODIPY)·*n*Solv supramolecular complexes (where Solv is a polar electron-donating solvent molecule) are analyzed based on the results of experimental studies and computational modeling.

2.2. Investigation of Supramolecular Complexes of **1–3** with Electron-Donating Solvents (Acetone, DMF, and DMSO)

The influence of the composition of benzene–electron-donor solvent (acetone, DMF, or DMSO) binary mixtures on the spectral characteristics of **1–3** was studied experimentally. Complexes **1**, **2**, and **3** fluoresce intensely in benzene, with emission band maxima at 583, 569, and 559 nm, and the fluorescence quantum yields are 87, 76, and 94%, respectively (Table S1). With an increase in the polar component (Solv) molar fraction (χ), the intense band maxima in the absorption spectra of **1–3** shift to the blue region (up to 9 nm), along with a decrease in the absorption intensity at the first band maximum (Figure S2). This may indicate the stabilization of the system, which has a higher dipole moment in the excited state compared to the ground state. An increase in the electron-donor concentration in mixtures with benzene is accompanied by a blue shift (up to 15 nm) of the emission band maxima of **1–3** (Figure S3). The effect of the fluorescence quenching of **1–3** is observed even

with small ($\chi = 0.2$ – 0.6) additions of the electron-donor quencher in the binary solvent. The intensity and Φ_f of **1–3** are close to the corresponding values in the electron donor at a higher mole fraction of the quencher in a binary solvent (Figures S2 and S3).

Complex **2** has fluorescence characteristics with the highest sensitivity to the presence of an electron donor, as in the case of alcohols (Figure S3) [29]. Compared to pure benzene in mixtures with a molar fraction of the electron donor $\chi = 0.3$, the Φ_f of **2** decreases by 6.7, 7.6, and 13.8 times in the presence of acetone, DMF, and DMSO, respectively (Figure S3b,e,h). The Φ_f of compounds **1** and **3** in mixtures similarly decreases by 5.1, 5.9, and 8.4 and 4.7, 5.0, and 6.8 times respectively (Figure S3a,c,d,f,g,i). The first confirmation of the presence of specific interactions between **1–3** and acetone, DMF, and DMSO molecules was studied using the Stern–Volmer equation of fluorescence quenching (Equation (1)):

$$I_0/I = 1 + K_{SV}[Solv] \quad (1)$$

where I and I_0 are the fluorescence intensities of **1–3** in the presence and absence of a quencher, respectively, K_{SV} is the fluorescence-quenching constant, and $[Solv]$ is the quencher concentration.

The linearity deviation of Stern–Volmer plots in benzene–electron-donor mixtures indicates that the fluorescence quenching of **1–3** is dynamic and static in nature (Figures 3 and S4).

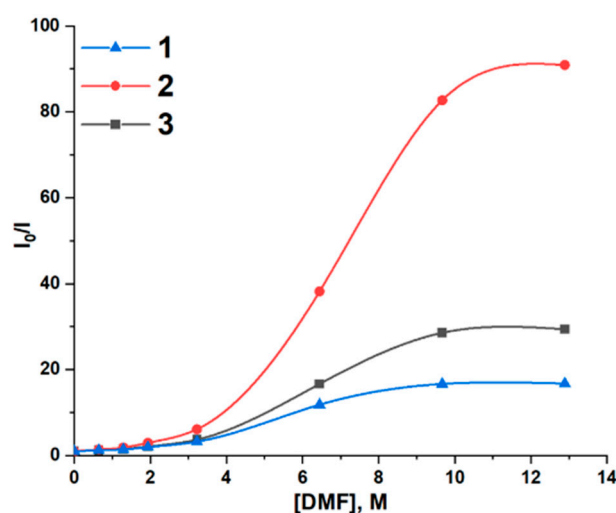


Figure 3. Stern–Volmer curves for fluorescence quenching of **1–3** ($c = 2.0 \cdot 10^{-6}$ mol/L) with the addition of various DMF concentrations.

K_{SV} was estimated from the linear plot of I_0/I vs. $[Solv]$ up to ~ 2.6 M of the quencher (Figures 4 and S5) in benzene–electron-donor systems. The analysis of the data obtained (Table 1; Figures 4 and S5) showed that K_{SV} values for **1–3** increase with an increase in the electron-donating ability in the series: acetone \rightarrow DMF \rightarrow DMSO.

The stability and composition of supramolecular structures of CH_2 -bis(BODIPY)s **1–3** were estimated from the results of UV/vis titration of **1–3** solutions in benzene–Solv (Solv: acetone, DMF, or DMSO). The stoichiometric composition of supramolecular complexes was determined from the slope of the graphical dependence $\lg[(I_q - I_0)/(I_\infty - I_0)]$ OT $\lg[Solv]$ (Equation (2)) [31].

$$K = \frac{(I_q - I_0)/(I_\infty - I_0)}{1 - (I_q - I_0)/(I_\infty - I_0)} \cdot \frac{1}{\left(c_q^0 - c_{[bis(\text{BODIPY})]}^0 \left(\frac{I_q - I_0}{I_\infty - I_0}\right)\right)^n} \quad (2)$$

where c_q^0 the initial concentration of the electron donor (Solv); $c_{[bis(\text{BODIPY})]}^0$ is the initial concentration of CH_2 -bis(BODIPY)s **1–3** in benzene; I_0 and I are **1–3**'s fluorescence intensities in

the absence and presence of the electron donor (Solv), respectively; I_∞ is 1–3's fluorescence intensity in a pure Solv quencher, and n is the stoichiometric coefficient.

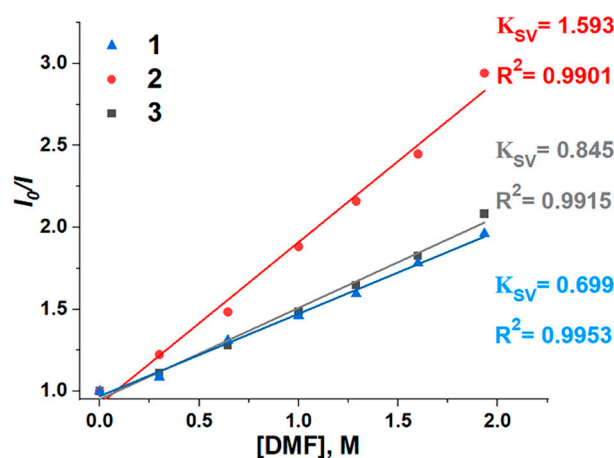


Figure 4. The linear fitting of the Stern–Volmer curve for the concentration range of DMF.

Table 1. The values of K_{SV} and $\lg K$ for CH_2 -bis(BODIPY)-2Solv supramolecular structures.

Solv	Luminophores		
	1	2	3
	$K_{SV}, \text{M}^{-1}; (\lg K)$		
Acetone	0.048 (2.7)	0.095 (4.2)	0.056 (3.5)
DMF	0.699 (4.7)	1.593 (5.0)	0.845 (4.8)
DMSO	1.913 (5.1)	4.211 (5.4)	2.590 (5.2)

Note: The error in determining $\lg K$ values from fluorometric titration data does not exceed 7–10%.

The data obtained (Figure S6) indicate that 1–3 form supramolecular structures with the electron-donating molecules with the stoichiometric composition CH_2 -bis(BODIPY)-2Solv, which is consistent with the results of quantum chemical calculations. To estimate the thermodynamic constants of supramolecular complexation processes, we used the modified Benesi–Hildebrand equation (Equation (3)), which is traditionally used to determine the thermodynamic constants of processes from spectrofluorimetric titration data:

$$(I_\infty - I_0) / (I_x - I_0) = 1 + (1/K)(1/[X]^n) \quad (3)$$

where I_0 and I_x are the fluorescence intensities of 1–3 in benzene in the absence and presence of Solv, respectively, I_∞ is the fluorescence intensity of 1–3 in a pure quencher, K_b is the binding constant, $[X]$ is the quencher concentration, and n is the stoichiometric coefficient.

The $\lg K$ values of CH_2 -bis(BODIPY)-2Solv range from 2.7 to 5.4 (Figures 5 and S7; Table 1). The results obtained indicate the relatively high stability of CH_2 -bis(BODIPY)-2Solv supramolecular structures with electron-donating analytes. The $\lg K$ values increase in the series $1 < 3 < 2$. (Table 1). This tendency is consistent with the regularity of the increase in the fluorescence sensitivity in the same series of 1–3. Based on the results of our research, which have already been published in earlier papers with supramolecular structures of 1–3 with alcohols [29], we analyzed the effect of the solvents' electron-donating ability on the fluorescence-quenching efficiency and the supramolecular structures' stability (Figure S8).

The quenching constants and the stability of CH_2 -bis(BODIPY)-2Solv supramolecular structures increase with the increase in the electron-donating power of the solvent, and their analysis is included in the text of the article (marked in yellow). The results obtained are consistent with the conclusion that the main contribution to fluorescence quenching is made by specific interactions of the dye with the molecules of electron-donor solvents. Obviously, the differences in the stability of the molecular complexes of CH_2 -bis(BODIPY)-2Solv should

be determined by the features of intermolecular and intramolecular interactions, which are discussed below based on the results of computational modeling.

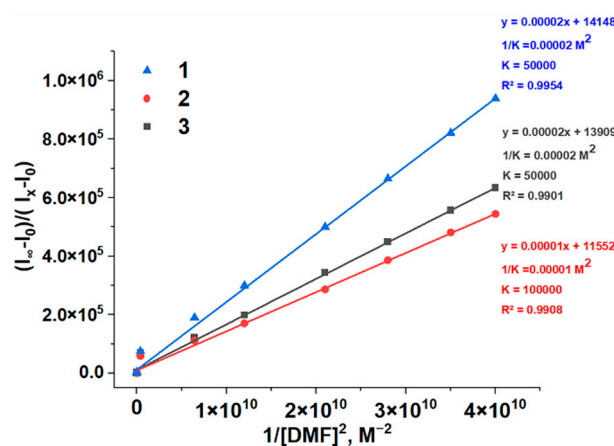


Figure 5. The Benesi–Hildebrand plots for determining the constants of additional coordination processes of 1–3 with DMF.

2.3. DFT Calculations

In Ref. [29], we demonstrated that CH₂-bis(BODIPY) fluorescence quenching in proton-donor solvents is due to photoinduced electron (charge) transfer in the composition of CH₂-bis(BODIPY)—nSolv supramolecular systems. In this study, using a similar DFT calculation algorithm and the example of CH₂-bis(BODIPY)s with acetone systems, we estimated the formation probability, composition, and structural features of CH₂-bis(BODIPY) supramolecular complexes with electron-donating molecules. Figure 6a schematically shows the CH₂-bis(BODIPY)·(acetone)_n (n = 1–4) systems' step-by-step formation mechanism, on the basis of which we determined their free energies of formation. An analysis of the free energy profiles shows that the most energetically favorable mechanism for CH₂-bis(BODIPY)s is the sequential addition of acetone molecules to CH₂-bis(BODIPY)s to form CH₂-bis(BODIPY)·2acetone supramolecular systems (Figure S9). Supramolecular complexes of CH₂-bis(BODIPY)·2acetone are formed through successive steps 1 and 2-2 by means of intermolecular contacts between the hydrogen atom of the methine spacer (H_{ms}) of each BODIPY moiety and the acetone oxygen atom (O_{solv}) (Figures 6b and S10). The H_{ms}···O_{solv} bond lengths are 2.687–3.108 Å (Figures 6 and S10; Table S4). The additional stabilization of these supramolecular systems is due to the presence of multipoint intermolecular contacts between the methyl moiety hydrogen atoms of the acetone molecule and one of the fluorine atoms of each BODIPY moiety. The free energy values confirm the thermodynamic stability of CH₂-bis(BODIPY)·2acetone supramolecular complexes (Figure S9).

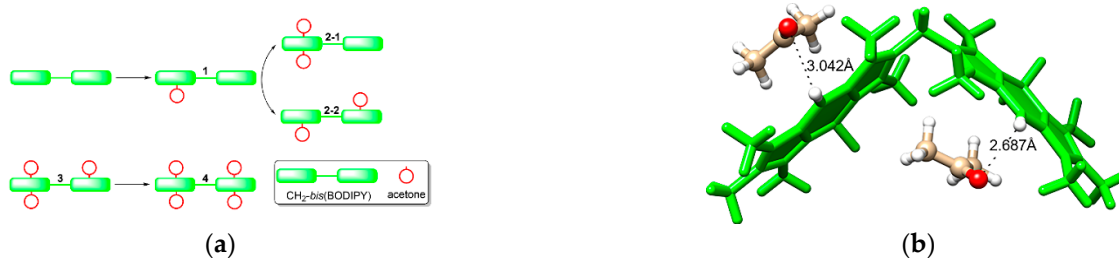


Figure 6. Schematic representation of the CH₂-bis(BODIPY)·2acetone formation mechanism (a) and optimized structure of 3,3'-CH₂-bis(BODIPY)·2acetone (b).

The results of TDDFT analysis made it possible to establish the effect of coordinated acetone molecules on the spectral properties of CH₂-bis(BODIPY)s. The TDDFT

spectra of CH₂-bis(BODIPY)s are interpreted in detail in Ref. [21]. As in the case of the initial CH₂-bis(BODIPY)s, in the TDDFT spectra of CH₂-bis(BODIPY)·2acetone, the two most intense bands are due to H (HOMO)–L (LUMO) and H–L+1 electronic transitions (Figure S11 and Table S5). However, in the case of 3,3'-CH₂-bis(BODIPY)·2acetone and 2,2'-CH₂-bis(BODIPY)·2acetone, a new electronically excited state is found in the higher-energy region (5.41 and 5.32 eV, respectively). The formation of this state is associated with H-8–L+1 and H-9–L electronic transitions. In 3,3'-CH₂-bis(BODIPY)·2acetone and 2,2'-CH₂-bis(BODIPY)·2acetone, the transfer occurs between donor and acceptor moieties located at a closer distance. Due to the lower symmetry of 2,3'-CH₂-bis(BODIPY), 2,3'-CH₂-bis(BODIPY)·2acetone is characterized by the formation of two new electronically excited states (H-8–L and H-9–L+1; 5.31 and 5.41 eV). In new electronically excited states, an electron density transfer from acetone as the electron donor moiety to CH₂-bis(BODIPY)·2acetone as the acceptor moiety is observed. It can be assumed that new low-lying electronically excited states are the result of ICT. Summarizing the results of the DFT study, we note that the fluorescence quenching of CH₂-bis(BODIPY)s in acetone's presence is associated with CH₂-bis(BODIPY)·2acetone formation, which increases the efficiency of non-radiative conversion and the implementation of ICT.

3. Materials and Methods

The compounds *bis*(1,2,3,7,8-pentamethyl-2,2'-dipyrrrolylmeten-9-yl)methane *bis*(difluoroborate) (**1**), (1,2,3,7,9-pentamethyl-2,2'-dipyrrrolylmeten-8-yl)-(1,2,3,7,8-pentamethyl-2,2'-dipyrrrolylmeten-9-yl)methane *bis*(difluoroborate) (**2**), and *bis*(1,2,3,7,9-pentamethyl-2,2'-dipyrrrolylmeten-8-yl)methane *bis*(difluoroborate) (**3**) were synthesized according to proven technology [21]. The synthesis techniques and the results of the identification of **1–3** are presented in SI. Spectrophotometric-grade benzene, heptane, cyclohexane, toluene, ethanol, 1-propanol, DMF, DMSO, and acetone (for analysis, Panreac, Barcelona) were used without further purification. Solvent parameters (*DN*, *SB*, and ϵ) were taken from [32] and are listed in Table S2.

3.1. Spectroscopic Experiments

Electronic absorption and fluorescence spectra of **1–3** solutions were recorded on a CM 2203 spectrometer (SOLAR) in the range of molar concentrations from 10^{−7} to 10^{−5} mol/L, and the thickness of the absorbing layer was 10 mm at $T = 25 \pm 0.1$ ° C. Fluorescence spectra were obtained at an optical density not higher than 0.1 at the excitation wavelength. The fluorescence quantum yields (Φ_f) of **1–3** were obtained [30] with Equation (4):

$$\Phi_{fx} = \Phi_{st}(A_{st}/A_x)(S_x/S_{st})(n_x/n_{st})^2 \quad (4)$$

where Φ_f is the fluorescence quantum yield of the substance (BODIPY), Φ_{st} is the fluorescence quantum yield of the standard (Rhodamine 6G, $\Phi_f = 94\%$ [33]), *S* is integrated fluorescence intensity (area under spectrum), *A* is absorbance at the excitation wavelength ($\lambda_{ex} = 520–525$ nm for **1–3**), and *n* is the refractive index.

Time-resolved fluorescence measurements were carried out by means of a high-performance fluorescence lifetime and steady-state spectrometer FluoTime 300 (PicoQuant, Germany) with an LDH-P-C-500 laser (PicoQuant, Germany) as an excitation source. The instrument response function (IRF) of the system was measured with the stray light signal of a dilute colloidal silica suspension (LUDOX®). The fluorescence decay curves were measured at the maxima of the emission peaks, and the fluorescence lifetimes were obtained by the reconvolution of the decay curves using the EasyTau 2 software package (PicoQuant, Germany). For nonpolar solvents (cyclohexane and benzene), the monoexponential decay model was applied. For polar electron-donating solvents (acetone, DMF, and DMSO), the biexponential fluorescence decay model was applied.

3.2. Computational Modeling

All calculations were carried out using Gaussian 16 [34]. To analyze the mechanism of CH₂-bis(BODIPY)-acetone system formation, geometry optimization and harmonic frequency calculations were performed with ω B97X-D/def2-TZVP [35,36]. The vertical electronic transitions were computed by the TDDFT method employing CAMB3LYP/def2-TZVP [37]. The SMD model [38] was applied to simulate the acetone medium. ChemCraft 1.8 (www.chemcraftprog.com, accessed on 30 October 2022) was used for analyses of results and molecular graphics.

4. Conclusions

The spectral properties and fluorescence quenching effect of CH₂-bis(BODIPY)s in polar electron-donating solvents (acetone, DMF, and DMSO) were analyzed in comparison with nonpolar solvents. The fluorescence quantum yield of 1–3 decreases from 0.99 in nonpolar cyclic and linear hydrocarbons and weakly polar chloroform to 0.008 in electron-donor organic solvents. In polar solvents, there is a complication of the law of fluorescence lifetime decay. The results show that for all dyes in nonpolar and weakly polar solvents, 1–3's total lifetime is noticeably higher (3.17–4.2 ns) than in acetone, DMF, and DMSO (0.44–1.30 ns). The high fluorescence sensitivity of CH₂-bis(BODIPY)s to the polarity, basicity, and electron-donating ability of solvents is due to CH₂-bis(BODIPY)·2Solv supramolecular structure formation. The values of the fluorescence-quenching constants (K_{SV}) of CH₂-bis(BODIPY)s 1–3 increase with the growth of the solvent's electron-donor properties: acetone → DMF → DMSO. The equilibrium constants (lgK) of the supramolecular complex formation processes, calculated using the modified Benesi–Hildebrand equation, are in the range from 2.7 to 5.4 and indicate the higher stability of CH₂-bis(BODIPY) supramolecular structures with electron-donating solvents compared to alcohols. The results form the basis for the development of fluorescent probes based on CH₂-bis(BODIPY)s for monitoring the complex parameter of the cellular structure polarity or the detection of electron-donating compounds (acetone, DMF, and DMSO) in solutions and biosystems.

Supplementary Materials: The are available online at <https://www.mdpi.com/article/10.3390/ijms232214402/s1>. References [21,29,32,39] are cited in the supplementary materials.

Author Contributions: Conceptualization, E.A.; methodology, E.A., M.B., and A.K. (Alexander Ksenofontov); validation, E.A., L.A., and M.B.; formal analysis, L.A.; investigation, A.K. (Alexander Kalyagin) and A.K. (Alexander Ksenofontov); resources, M.B.; data curation, E.A.; writing—original draft preparation, A.K. (Alexander Kalyagin) and A.K. (Alexander Ksenofontov); writing—review and editing, A.K. (Alexander Kalyagin), L.A., and A.K. (Alexander Ksenofontov); visualization, A.K. (Alexander Kalyagin) and A.K. (Alexander Ksenofontov); supervision, E.A.; funding acquisition, A.K. (Alexander Ksenofontov). All authors have read and agreed to the published version of the manuscript.

Funding: This work was supported by the state assignment of the Ministry of Science and Higher Education of the Russian Federation “Development of approaches and methods of physical chemistry in the study of multicomponent supramolecular, molecular and ion-molecular systems as promising materials”, No. AAAA-A21-121011490059-5 (synthesis and spectral characteristics of compounds). This work was supported by a grant from the Ministry of Science and Higher Education of the Russian Federation (No. 075-15-2021-579) (computational modeling).

Institutional Review Board Statement: Not applicable.

Informed Consent Statement: Not applicable.

Data Availability Statement: The raw data supporting the conclusions of this article will be made available by the authors, without undue reservation.

Acknowledgments: This work was carried out with the help of the Center for Collective Use of Scientific Equipment, “The upper Volga region center of physic-chemical research”.

Conflicts of Interest: The authors declare no conflict of interest related to this work.

References

1. Chaturvedi, P.; Majumder, S.K.; Krishna, H.; Muttagi, S.; Gupta, P.K. Fluorescence spectroscopy for noninvasive early diagnosis of oral mucosal malignant and potentially malignant lesions. *J. Cancer Res. Ther.* **2010**, *6*, 497–502. [[CrossRef](#)] [[PubMed](#)]
2. Francisco, A.L.N.; Correr, W.R.; Azevedo, L.H.; Kern, V.G.; Pinto, C.A.L.; Kowalski, L.P.; Kurachi, C. Fluorescence spectroscopy for the detection of potentially malignant disorders and squamous cell carcinoma of the oral cavity. *Photodiagnosis Photodyn. Ther.* **2014**, *11*, 82–90. [[CrossRef](#)] [[PubMed](#)]
3. Kaniyala Melanthota, S.; Kistenev, Y.V.; Borisova, E.; Ivanov, D.; Zakharova, O.; Boyko, A.; Vrazhnov, D.; Gopal, D.; Chakrabarti, S.; K, S.P.; et al. Types of spectroscopy and microscopy techniques for cancer diagnosis: A review. *Lasers Med. Sci.* **2022**, *37*, 3067–3084. [[CrossRef](#)]
4. Ramanujam, N. Fluorescence spectroscopy of neoplastic and non-neoplastic tissues. *Neoplasia* **2000**, *2*, 89–117. [[CrossRef](#)] [[PubMed](#)]
5. Wan, Q.-S.; Wang, T.; Zhang, K.-H. Biomedical optical spectroscopy for the early diagnosis of gastrointestinal neoplasms. *Tumour Biol.* **2017**, *39*, 1010428317717984. [[CrossRef](#)]
6. Lu, P.; Chung, K.-Y.; Stafford, A.; Kiker, M.; Kafle, K.; Page, Z.A. Boron dipyrromethene (BODIPY) in polymer chemistry. *Polym. Chem.* **2021**, *12*, 327–348. [[CrossRef](#)]
7. Lin, W.; Colombani-Garay, D.; Huang, L.; Duan, C.; Han, G. Tailoring nanoparticles based on boron dipyrromethene for cancer imaging and therapy. *WIREs Nanomed. Nanobiotechnol.* **2020**, *12*, e1627. [[CrossRef](#)] [[PubMed](#)]
8. Kue, C.S.; Ng, S.Y.; Voon, S.H.; Kamkaew, A.; Chung, L.Y.; Kiew, L.V.; Lee, H.B. Recent strategies to improve boron dipyrromethene (BODIPY) for photodynamic cancer therapy: An updated review. *Photochem. Photobiol. Sci.* **2018**, *17*, 1691–1708. [[CrossRef](#)] [[PubMed](#)]
9. Loudet, A.; Burgess, K. BODIPY dyes and their derivatives: Syntheses and spectroscopic properties. *Chem. Rev.* **2007**, *107*, 4891–4932. [[CrossRef](#)]
10. Requena, S.; Ponomarchuk, O.; Castillo, M.; Rebik, J.; Brochiero, E.; Borejdo, J.; Gryczynski, I.; Dzyuba, S.V.; Gryczynski, Z.; Grygorczyk, R.; et al. Imaging viscosity of intragranular mucin matrix in cystic fibrosis cells. *Sci. Rep.* **2017**, *7*, 16761. [[CrossRef](#)]
11. Raut, S.L.; Kimball, J.D.; Fudala, R.; Bora, I.; Chib, R.; Jaafari, H.; Castillo, M.K.; Smith, N.W.; Gryczynski, I.; Dzyuba, S.V.; et al. A triazine-based BODIPY trimer as a molecular viscometer. *Phys. Chem. Chem. Phys.* **2016**, *18*, 4535–4540. [[CrossRef](#)]
12. Kimball, J.D.; Raut, S.; Jameson, L.P.; Smith, N.W.; Gryczynski, Z.; Dzyuba, S.V. BODIPY-BODIPY dyad: Assessing the potential as a viscometer for molecular and ionic liquids. *RSC Adv.* **2015**, *5*, 19508–19511. [[CrossRef](#)] [[PubMed](#)]
13. Bumagina, N.A.; Antina, E.V.; Ksenofontov, A.A.; Antina, L.A.; Kalyagin, A.A.; Berezin, M.B. Basic structural modifications for improving the practical properties of BODIPY. *Coord. Chem. Rev.* **2022**, *469*, 214684. [[CrossRef](#)]
14. Ravikanth, M.; Vellanki, L.; Sharma, R. Functionalized boron-dipyrromethenes and their applications. *Rep. Org. Chem.* **2016**, *6*, 1. [[CrossRef](#)]
15. Xiao, H.; Li, P.; Tang, B. Recent progresses in fluorescent probes for detection of polarity. *Coord. Chem. Rev.* **2021**, *427*, 213582. [[CrossRef](#)]
16. Saremi, B.; Bandi, V.; Kazemi, S.; Hong, Y.; D'Souza, F.; Yuan, B. Exploring NIR Aza-BODIPY-Based Polarity Sensitive Probes with ON-and-OFF Fluorescence Switching in Pluronic Nanoparticles. *Polymers* **2020**, *12*, 540. [[CrossRef](#)]
17. Squeo, B.M.; Pasini, M. BODIPY platform: A tunable tool for green to NIR OLEDs. *Supramol. Chem.* **2020**, *32*, 56–70. [[CrossRef](#)]
18. Ivaniuk, K.; Pidluzhna, A.; Stakhira, P.; Baryshnikov, G.V.; Kovtun, Y.P.; Hotra, Z.; Minaev, B.F.; Ågren, H. BODIPY-core 1,7-diphenyl-substituted derivatives for photovoltaics and OLED applications. *Dye. Pigment.* **2020**, *175*, 108123. [[CrossRef](#)]
19. Bi, J.; Ji, X.; Guo, M.; Guo, H.; Yang, F. A fluorescent sensor for thymine based on bis-BODIPY containing butanediamido bridges. *New J. Chem.* **2019**, *43*, 5890–5896. [[CrossRef](#)]
20. Boens, N.; Leen, V.; Dehaen, W. Fluorescent indicators based on BODIPY. *Chem. Soc. Rev.* **2012**, *41*, 1130–1172. [[CrossRef](#)]
21. Antina, L.A.; Ksenofontov, A.A.; Kalyagin, A.A.; Antina, E.V.; Berezin, M.B.; Khodov, I.A. Luminescent properties of new 2,2-, 2,3- and 3,3-CH₂-bis(BODIPY)s dyes: Structural and solvation effects. *Spectrochim. Acta Part A Mol. Biomol. Spectrosc.* **2019**, *218*, 308–319. [[CrossRef](#)] [[PubMed](#)]
22. Ksenofontov, A.A.; Guseva, G.B.; Antina, E.V.; V'yugin, A.I. Molecular structure of bis(dipyrrolyl)methanates of d-metals according to the quantum chemical calculations by the PM6 method. *J. Struct. Chem.* **2014**, *55*, 418–423. [[CrossRef](#)]
23. Ksenofontov, A.A.; Antina, E.V.; Guseva, G.B.; Berezin, M.B.; Antina, L.A.; Vyugin, A.I. Prospects of applications of fluorescent sensors based on zinc(II) and boron(III) bis(dipyrromethenates). *J. Mol. Liq.* **2019**, *274*, 681–689. [[CrossRef](#)]
24. Ksenofontov, A.A.; Guseva, G.B.; Antina, E.V.; Nuraneeva, E.N. «On-off» fluorescent sensors for aromatic analytes based on zinc(II) bis(dipyrromethenates). *Spectrochim. Acta Part A Mol. Biomol. Spectrosc.* **2017**, *173*, 222–227. [[CrossRef](#)] [[PubMed](#)]
25. Ahrens, J.; Cordes, B.; Wicht, R.; Wolfram, B.; Bröring, M. Acidic Condensation of BODIPYs with Aldehydes: A Quick and Versatile Route to Alkenyl-BODIPYs and C(sp³)-Connected DYEmers. *Chemistry* **2016**, *22*, 10320–10325. [[CrossRef](#)]
26. Bröring, M.; Krüger, R.; Link, S.; Kleeberg, C.; Köhler, S.; Xie, X.; Ventura, B.; Flamigni, L. Bis(BF₂)-2,2'-bidipyrrens (BisBODIPYs): Highly fluorescent BODIPY dimers with large Stokes shifts. *Chemistry* **2008**, *14*, 2976–2983. [[CrossRef](#)]
27. Ventura, B.; Marconi, G.; Bröring, M.; Krüger, R.; Flamigni, L. Bis(BF₂)-2,2'-bidipyrrens, a class of BODIPY dyes with new spectroscopic and photophysical properties. *New J. Chem.* **2009**, *33*, 428–438. [[CrossRef](#)]
28. Zhang, X.-F.; Yang, X.; Xu, B. PET-based bisBODIPY photosensitizers for highly efficient excited triplet state and singlet oxygen generation: Tuning photosensitizing ability by dihedral angles. *Phys. Chem. Chem. Phys.* **2017**, *19*, 24792–24804. [[CrossRef](#)]

29. Antina, L.A.; Kalyagin, A.A.; Ksenofontov, A.A.; Pavelyev, R.S.; Lodochnikova, O.A.; Islamov, D.R.; Antina, E.V.; Berezin, M.B. Effect of polar protic solvents on the photophysical properties of bis(BODIPY) dyes. *J. Mol. Liq.* **2021**, *337*, 116416. [[CrossRef](#)]
30. Lakowicz, J.R. *Principles of Fluorescence Spectroscopy*, 3rd ed.; Springer: New York, NY, USA, 2006; ISBN 978-0-387-46312-4.
31. Lee, S.-C.; Heo, J.; Woo, H.C.; Lee, J.-A.; Seo, Y.H.; Lee, C.-L.; Kim, S.; Kwon, O.-P. Fluorescent Molecular Rotors for Viscosity Sensors. *Chemistry* **2018**, *24*, 13706–13718. [[CrossRef](#)]
32. Haidekker, M.A.; Brady, T.P.; Lichlyter, D.; Theodorakis, E.A. Effects of solvent polarity and solvent viscosity on the fluorescent properties of molecular rotors and related probes. *Bioorganic Chem.* **2005**, *33*, 415–425. [[CrossRef](#)] [[PubMed](#)]
33. Fischer, M.; Georges, J. Fluorescence quantum yield of rhodamine 6G in ethanol as a function of concentration using thermal lens spectrometry. *Chem. Phys. Lett.* **1996**, *260*, 115–118. [[CrossRef](#)]
34. Frisch, M.J.; Trucks, G.W.; Schlegel, H.B.; Scuseria, G.E.; Robb, M.A.; Cheeseman, J.R.; Scalmani, G.; Barone, V.; Petersson, G.A.; Nakatsuji, H.; et al. *Gaussian 16, Revision C.01*; Gaussian, Inc.: Wallingford, CT, USA, 2016.
35. Chai, J.-D.; Head-Gordon, M. Long-range corrected hybrid density functionals with damped atom-atom dispersion corrections. *Phys. Chem. Chem. Phys.* **2008**, *10*, 6615–6620. [[CrossRef](#)]
36. Weigend, F.; Ahlrichs, R. Balanced basis sets of split valence, triple zeta valence and quadruple zeta valence quality for H to Rn: Design and assessment of accuracy. *Phys. Chem. Chem. Phys.* **2005**, *7*, 3297–3305. [[CrossRef](#)] [[PubMed](#)]
37. Yanai, T.; Tew, D.P.; Handy, N.C. A new hybrid exchange–correlation functional using the Coulomb-attenuating method (CAM-B3LYP). *Chem. Phys. Lett.* **2004**, *393*, 51–57. [[CrossRef](#)]
38. Marenich, A.V.; Cramer, C.J.; Truhlar, D.G. Universal solvation model based on solute electron density and on a continuum model of the solvent defined by the bulk dielectric constant and atomic surface tensions. *J. Phys. Chem. B* **2009**, *113*, 6378–6396. [[CrossRef](#)]
39. Riddick, J.A.; Bunger, W.B.; Sakano, T.K. *Organic solvents: Physical properties and methods of purification*, 4th ed.; Riddick, J.A., Bunger, W.B., Sakano, T.K., Eds.; Wiley: New York, NY, USA; Chichester, UK, 1986; ISBN 978-0471084679.